PROCEEDINGS OF SCIENCE

Performance of Missing Energy reconstruction at the CMS detector in 13 TeV data

Robert Schöfbeck on behalf of the CMS collaboration*
Ghent University
E-mail: robert.schoefbeck@cern.ch

The precise understanding of the missing transverse momentum observable is crucial for searches for processes beyond the Standard Model as well as for precision measurements. The high collision rate at the CMS detector during the 13 TeV data-taking periods of the LHC poses challenges to reconstruction far beyond those previously overcome. I will review the performance of missing energy in LHC Run-II data and discuss results on advanced reconstruction algorithms which mitigate the effects of pileup collisions.

38th International Conference on High Energy Physics
3-10 August 2016
Chicago, USA

*Speaker.

PoS(ICHEP2016)291

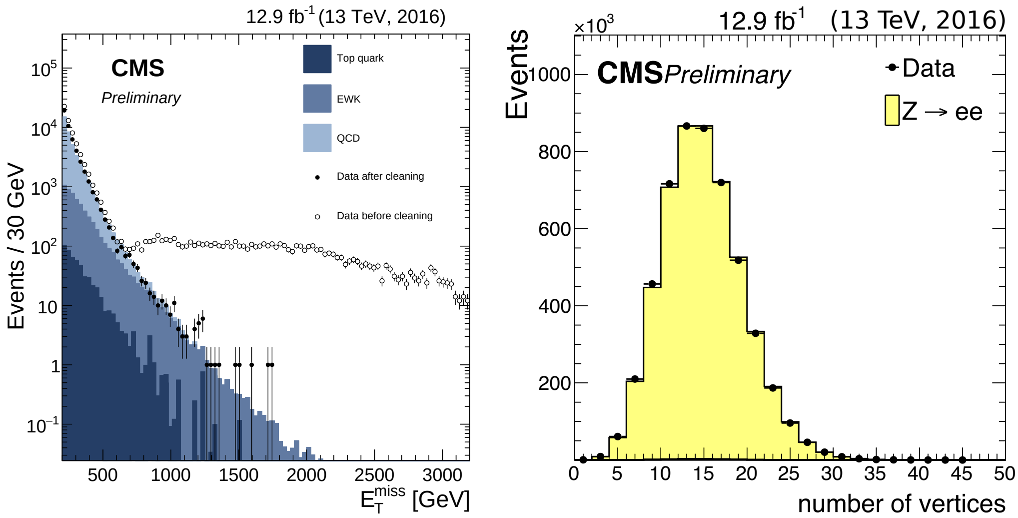

Figure 1: The E_T^{miss} distributions for events passing the dijet selection with the 2016 cleaning algorithms applied including the one based on jet identification requirements (left, filled markers), without the 2016 cleaning algorithms applied (open markers), and from simulation (filled histograms). The top quark contribution corresponds to the top pair and single-top production processes. The EWK contribution corresponds to $Z \to ll$, $Z \to \nu\nu$, $W \to l\nu$ and diboson processes. Multiplicity of reconstructed vertices for $Z \to e^+e^-$candidate events (right).

1. Introduction

The CMS detector [1] can detect almost all stable or long-lived particles produced in the proton-proton (pp) collisions provided by the LHC at CERN. Notable exceptions are neutrinos and hypothetical neutral weakly interacting particles. Although these particles do not leave a signal in the detector, their presence can be inferred from the momentum imbalance in the plane perpendicular to the beam direction, a quantity known as missing transverse momentum and denoted by $\vec{E}_T^{miss}$. Its magnitude is denoted by E_T^{miss} and will be referred to as missing transverse energy.

Beyond the imperfect resolution of all detectable and reconstructed physics objects (e, μ, τ, γ, jets, etc), the E_T^{miss} measurement is sensitive to overlapping detector signals from additional interactions in the previous, the same, or subsequent bunch crossings (commonly referred to as in-time and out-of-time pileup), particle misidentification, as well as detector malfunctions. In this note, I summarize the performance of E_T^{miss} reconstruction in 13 TeV pp collision data [2] and the efforts to mitigate the effects of pileup. Previous studies of the missing transverse energy reconstruction in 7 and 8 TeV data were presented in [3, 4].

2. Cleaning of the E_T^{miss} tail

In order to study anomalous high-E_T^{miss} events, we select an event sample collected with a hadronic energy sum trigger, that requires total hadronic energy in the event to be larger than 800 GeV. Subsequently, dijet events are selected by requiring a leading jet with $p_T > 400$ GeV and at least one more jet with $p_T > 200$ GeV. Events with an identified photon, electron or muon

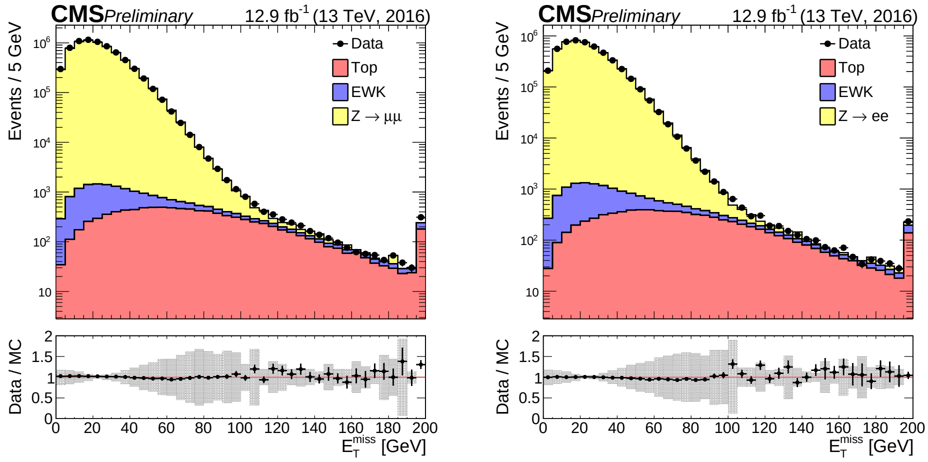

Figure 2: Distributions of $E_{\mathrm{T}}^{\mathrm{miss}}$ in $\mathrm{Z} \to \mu^+\mu^-$(left) and $\mathrm{Z} \to e^+e^-$(right). The points in the lower panel of each plot show the data/MC ratio, including the statistical uncertainties of both data and simulation. The systematic uncertainty due to the jet energy corrections and the systematic uncertainty in the unclustered energy is also displayed on the ratio. The last bin contains overflow content. The top contribution corresponds to the top pair and single top production processes. The EWK contribution corresponds to the diboson, $\mathrm{Z}\gamma$ and $\mathrm{W}\gamma$ production processes.

are rejected. The resulting $E_{\mathrm{T}}^{\mathrm{miss}}$ distribution is shown in Fig. 1. Various sources contributing to the high-$E_{\mathrm{T}}^{\mathrm{miss}}$ tail have been identified. In the the electromagnetic calorimeter (ECAL), spurious deposits may appear due to high-energetic particles that strike sensors directly. Moreover, ECAL dead cells can lead to a biased energy measurement of the electromagnetic component of a shower. The hadronic calorimeter (HCAL), is subject to noise in the hybrid photo diode (HPD) and readout box (RBX) electronics, as well as direct particle interactions with the light guides and photomultiplier tubes of the forward calorimeter. Furthermore, machine-induced backgrounds, such as the production of muons when beam protons undergo collisions upstream of the detector (beam halo), can cause high-$E_{\mathrm{T}}^{\mathrm{miss}}$ signatures that are unrelated to the hard scattering in the collision event. These beam halo particles will travel nearly parallel to the collision axis and will leave a calorimeter deposit along a line at constant ϕ in the calorimeter. Event filters based on topological and timing information of the spurious signals have been developed and tested during the 2010 and 2012 LHC running period [3, 4] and were updated to the 25 ns bunch spacing conditions of the LHC in the 13 TeV data taking period. The combined effect of these cleaning algorithms brings the dijet data in Fig. 1 in agreement with simulation over several orders of magnitude with essentially no residual tail up to the TeV range.

The multiplicity of reconstructed vertices is also shown in Fig. 1. This quantity is closely correlated with pileup and, in turn, affects $E_{\mathrm{T}}^{\mathrm{miss}}$ performance in the bulk of the events, which we study in the next section.

3. $E_{\mathrm{T}}^{\mathrm{miss}}$ response and resolution

Unavoidable deficiencies in the event reconstruction, such as energy thresholds in the calorimeters, inefficiencies in the tracker, and nonlinearity of the response of the calorimeter for hadronic

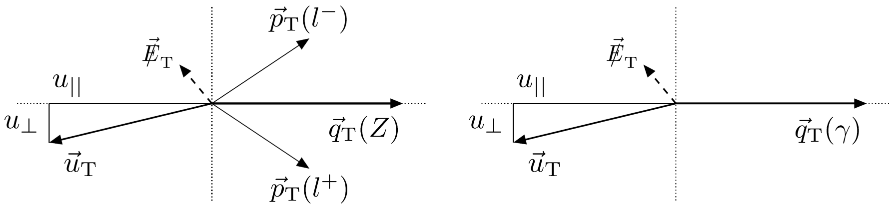

Figure 3: Illustration of $Z \to \ell^+\ell^-$ (left) and photon (right) event kinematics in the transverse plane. The vector $\vec{u}_T$ denotes the vectorial sum of all particles reconstructed in the event except for the two leptons from the Z decay (left) or the photon (right).

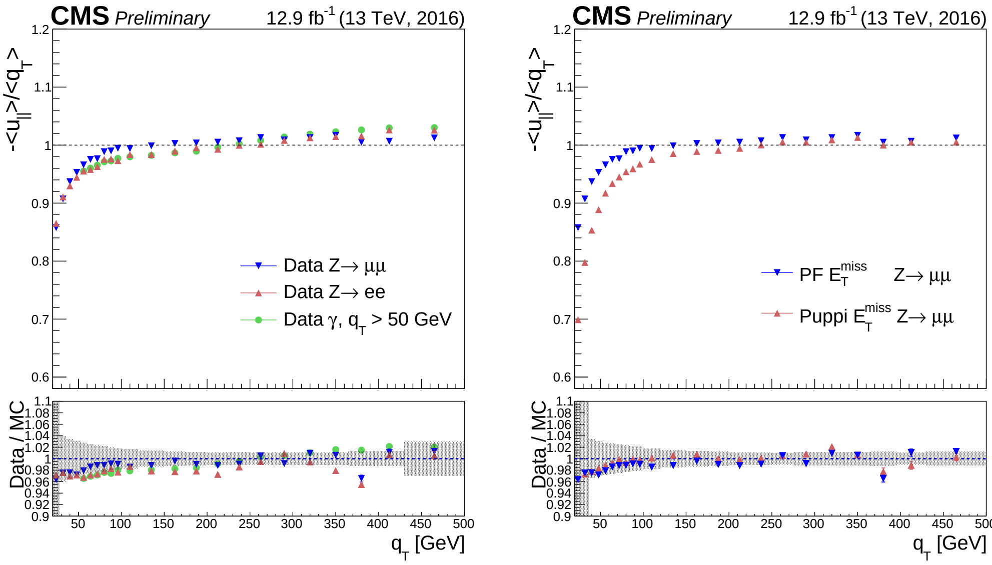

Figure 4: Response is shown for $Z \to \mu^+\mu^-$events, $Z \to e^+e^-$events and γ events for PF E_T^{miss} (left) and in comparison to Puppi E_T^{miss} (right). The upper frame shows the response in data; the lower frame shows the ratio of data to simulation with the error band displaying the systematic uncertainty of the simulation, estimated as the $Z \to e^+e^-$channel systematic uncertainty.

particles, can lead to a bias of the E_T^{miss} measurement. It is strongly reduced, however, by correcting the p_T of the jets to the particle level jet p_T using the jet energy corrections [5] and propagating the correction into the $\vec{E}_T^{miss}$. Scale and resolution of E_T^{miss} evaluated after performing these corrections can be studied in events with a well-identified Z boson or an isolated photon. Momenta of muons, electrons and photons are reconstructed with high resolution (1-6%) [6, 7], whereas jets are reconstructed with less precision [5]. Consequently, the E_T^{miss} resolution in Z or γ + jets events is dominated by the hadronic activity in the event. The E_T^{miss} distributions in $Z \to \mu^+\mu^-$ and $Z \to e^+e^-$ events are presented in Fig. 2. The data distributions are modeled well by the simulation. The increase in the uncertainty band in Fig. 2 around 60 GeV is due to the large impact of the uncertainty on deposits reconstructed as hadrons that were not clustered in a jet, a contribution that is particularly relevant in low energetic Drell-Yan events with no genuine E_T^{miss}.

Figure 3 depicts how vector boson momenta are used study E_T^{miss} performance in the recoiling system. The vector boson momentum in the transverse plane is denoted by $\vec{q}_T$, and the transverse

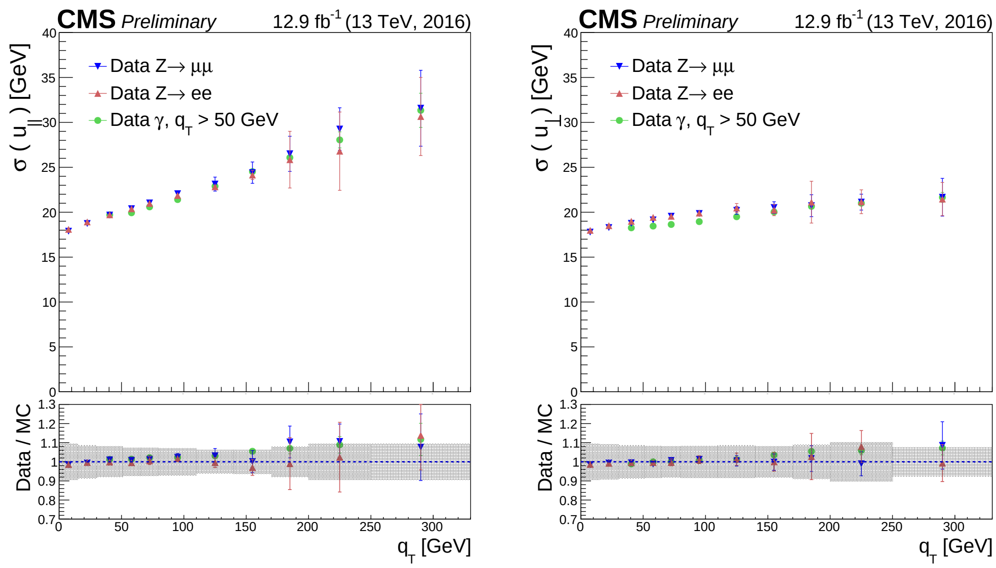

Figure 5: Resolution is shown for $Z \to \mu^+\mu^-$events, $Z \to e^+e^-$events and γ events. The upper frame shows the resolution in data; the lower frame shows the ratio of data to simulation with the error band displaying the systematic uncertainty of the simulation, estimated as the $Z \to e^+e^-$channel systematic uncertainty.

momentum of the hadronic recoil, defined as the vectorial sum of the transverse momenta of all particles except the vector boson or its decay products, is denoted by $\vec{u}_T$. Momentum conservation in the transverse plane dictates that $\vec{q}_T + \vec{u}_T + \vec{E}_T = 0$. Projecting this vectorial equation on the vector boson direction and orthogonal to it defines $u_\parallel$ and $u_\perp$. Using a Voigtian parametrization [4], we can measure the E_T^{miss} response by $-\langle u_\parallel \rangle / \langle q_T \rangle$ whereas the resolution of the hadronic recoil component parallel and orthogonal to the reference vector boson momentum is given by $\sigma(u_\parallel + q_T)$ and $\sigma(u_\perp)$.

In order to improve reconstruction performance and mitigate the effects of pileup collisions, new techniques have been developed to reduce the pileup dependence of jets and E_T^{miss}. One of these techniques is pileup per particle identification (PUPPI) [8, 2] and attempts to use information on neighboring particles to infer a probability that a given particle is from a pileup collision.

Figure 4 shows the response curves as a function of q_T, extracted from data and simulation in $Z \to \mu^+\mu^-$, $Z \to e^+e^-$, and photon events. Good agreement is observed between the data and simulation in all three different final states and E_T^{miss} fully recovers the hadronic recoil activity for Z boson momenta in excess of 50 GeV. The response in data and simulation is in agreement well within the uncertainties. Comparing nominal E_T^{miss} response with PUPPI E_T^{miss} response exhibits a 4% difference in $Z \to \mu^+\mu^-$ events at low q_T attributed to an over-removal of pileup candidates from the event. This latter effect is corrected for particles that are clustered to jets, however, the unclustered energy is not separately corrected, and hence the over-removal is most visible at low q_T.

Finally, Figs. 5,6 show the resolution curves as a function of q_T for $u_\parallel$ and $u_\perp$. For nominal E_T^{miss}, there is good agreement between data and simulation for $Z \to \mu^+\mu^-$, $Z \to e^+e^-$, and photon events and the resolution for the component parallel to the vector boson momentum rises approximately linearly in the accessible range. The isotropic nature of the perpendicular compo-

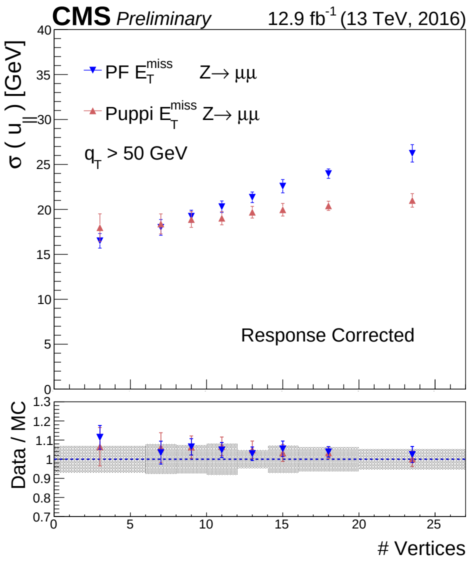

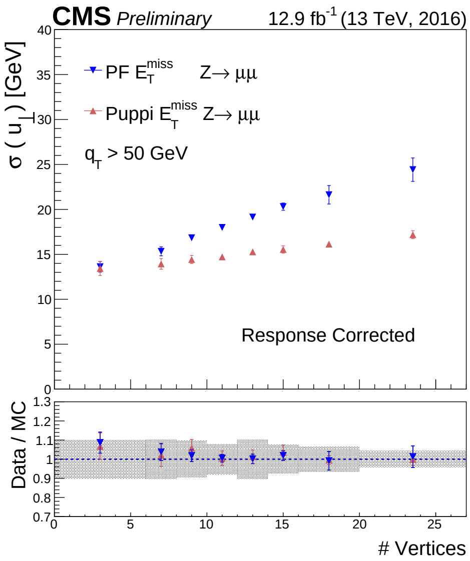

Figure 6: Resolution is shown for $Z \to \mu^+\mu^-$events. The upper frame shows the resolution in data for $E_{\mathrm{T}}^{\mathrm{miss}}$ (red triangle) and PUPPI $E_{\mathrm{T}}^{\mathrm{miss}}$ (blue triangle); the lower frame shows the ratio of data to simulation with the error band displaying the systematic uncertainty of the simulation.

nent causes its resolution to have a reduced dependence on q_{T}. Because the 4% reduction of PUPPI $E_{\mathrm{T}}^{\mathrm{miss}}$ response is significant, the resolution in Fig. 6 is corrected for this effect. Both, the parallel and perpendicular component show a greatly improved dependence on vertex multiplicity when compared to nominal $E_{\mathrm{T}}^{\mathrm{miss}}$.

4. Conclusion

We study missing transverse energy performance in pp collision data collected with the CMS detector in 2016 at 13 TeV, corresponding to an integrated luminosity up to 12.9 fb^{-1}. Noise cleaning algorithms in dijet events show excellent performance. Comparing reconstructed $E_{\mathrm{T}}^{\mathrm{miss}}$ to the vector boson momentum in events with no genuine $E_{\mathrm{T}}^{\mathrm{miss}}$, we establish agreement with expectations from the simulation and stability with respect to pileup activity for both $E_{\mathrm{T}}^{\mathrm{miss}}$ response and resolution. The novel PUPPI algorithm moreover achieves a significant reduction of the dependence on pileup. In summary, the performance of missing energy reconstruction at CMS provides a solid foundation for future CMS measurements.

References

[1] CMS collaboration, *"The CMS experiment at the CERN LHC"*, **JINST** 3 (2008) S08004, doi:10.1088/1748-0221/3/08/S08004.

[2] CMS collaboration, *"Performance of missing energy reconstruction in 13 TeV pp collision data using the CMS detector"*, **CMS Physics Analysis Summary**, http://cds.cern.ch/record/2205284

[3] CMS collaboration, *"Missing transverse energy performance of the CMS detector"*, **JINST** 6 (2011) P09001, doi:0.1088/1748-0221/6/09/P09001.

[4] CMS collaboration,*"Performance of the CMS missing transverse momentum reconstruction in pp data at $\sqrt{s}$ = 8 TeV"*, **JINST 10/02 (2015) P02006** , doi:10.1088/1748-0221/10/02/P02006.

[5] CMS collaboration,*"Jet energy scale and resolution in the CMS experiment in pp collisions at 8 TeV"*, submitted to **JINST**, http://cds.cern.ch/record/2198719.

[6] CMS collaboration,*"Performance of CMS muon reconstruction in pp collision events at $\sqrt{s} = 7\,TeV$"*, **JINST** 7 (2012) P10002, doi:10.1088/1748-0221/7/10/P10002.

[7] CMS collaboration,*"Performance of Photon Reconstruction and Identification with the CMS Detector in Proton-Proton Collisions at sqrts = 8 TeV"*, **JINST** 10 (2014) P08010, doi:10.1088/1748-0221/10/08/P08010.

[8] Bertolini, Daniele and Harris, Philip and Low, Matthew and Tran, Nhan, *"Pileup Per Particle Identification"*, **JHEP** 10 (2015) 059, doi:10.1007/JHEP10(2014)059.